© Universiti Tun Hussein Onn Malaysia Publisher's Office

IJIE

Journal homepage: http://penerbit.uthm.edu.my/ojs/index.php/ijie
ISSN : 2229-838X e-ISSN : 2600-7916

The International Journal of Integrated Engineering

Comparison of BCH Code Performance in LTE-Advanced Cooperative System in Suburban, Urban and Rural Environment Based on WINNER II Channel Model

Mohammed Fadhil[1], Asma Abu-Samah[1], Rosdiadee Nordin[1*], Mahamod Ismail[1], Nor Fadzilah Abdullah[1]

[1]Department of Electrical, Electronic & Systems Engineering, Faculty of Engineering and Built Environment, Universiti Kebangsaan Malaysia, 43600 UKM Bangi, Selangor, MALAYSIA

*Corresponding Author

DOI: https://doi.org/10.30880/ijie.2021.13.05.027
Received 06 July 2020; Accepted 11 August 2021; Available online 24 November 2021

Abstract: Multi-path fading is a severe issue that causes fluctuations in the amplitudes of the received signals. For combating this issue, several researchers have used cooperative communication in the Long-Term Evolution (LTE)-advanced system. To further decrease the degradative effects of transmitted signals, various error correction techniques can be used to recover the erroneous components, especially when the channel has been deep fading. The paper investigates the general performance of the Convolutional Codes (CC) in the LTE-advanced cooperative system and compare it with the Bose-Chaudhuri-Hocquenghem (BCH) codes. The comparison is based on WINNER II project as the channel model between the nodes in the two coding processes. To validate the advantages of BCH code, the process were tested on three different environments; a suburban macro-cell, urban macro-cell, and the rural micro-cell with prior study to understand the appropriate relay height in every environment. Path loss models for each environment were derived and proposed as part of the proposed simulation framework. Conducted simulation studies based on bit error rate and direct connection showed that the use of the CC and the BCH codes in a relay technologies could significantly increase the system performance. It was noted that the performance of the system which used BCH nodes was better than the system using CC nodes in an LTE-advanced cooperative system.

Keywords: Bose-Chaudhuri-Hocquenghem (BCH), cooperative communication, LTE-Advanced, WINNER II

1. Introduction

Multiple-Input-Multiple-Output (MIMO) processes have been studied to provide reliable transmission information for higher data rate applications [1, 2]. Cooperative systems are a cost-effective and alternative system as they present similar diversity benefits like the centralised MIMO techniques using cooperation concept, but without increasing the power transmission. The cooperative communication system is a concept that can generate independent paths between the customer and Base Station (BS) using a new relay channel. This relay channel is regarded as the auxiliary channel to between the destination and source. The principal concept underlying the cooperation is the pool of resources between users in the network pool to develop a virtual antenna array for spatial diversity. The cooperative spatial diversity causes an increase in the exponential decay rate with regards to the error probability with an increase in the Signal-to-Noise Ratio (SNR).

In the past few years, the traditional relay has emerged as a major issue because this approach uses a system consisting of intermediate nodes, i.e., Relay Nodes (RN), that decode and forward the message received from the source. Though this technique is a very effective approach that saves energy owing to a nonlinear path loss, it is plagued by signal fading for individual links. This issue can be resolved by exploiting the existing differences, like frequency, time, and spatial diversity. For making use of the existing frequency and time diversities, several researchers have applied various channel codes like Turbo, Cyclic Redundancy Check, Low-Density Parity Check (LDPC) [3], convolutional, and the recently-reported Reed Solomon (RS) codes. The popular cooperative schemes include the Decoding and Forward (DF)

*Corresponding author: adee@ukm.edu.my

and the coded cooperation. One study used Convolutional Codes (CC) based on many wireless communication standards [4], and another [5] considered cooperative systems which used channel coding. In the latter, the active transmitting users codewords were split and transmitted to the independent fading channels. Researchers in [6] investigated the serial concatenated convolutional coding scheme performance against the flat fading channels by deliberating over the altered and delayed auditory feedback (DAF) cooperation.

Based on the literature review, existing works on Code-Division Multiple Access (CDMA) systems either adopt the assumption of orthogonal subchannels [7-9] or have considered synchronous communications [10,11]. Furthermore, [12] investigated the performance of the CDMA in the Cooperative Communication System, which used the Maximum Ratio Combiner (MRC) and the Equal Gain Combiner (EGC). Bose-Chaudhuri-Hocquenghem (BCH) codes were suggested to be a superior code error correction technique [13], but only a few studies have employed the BCH code in the cooperative system. Existing studies consider either direct link communication [14] or cooperation in sensor network systems [15,16]. This paper aims to prove BCH's potential to further reduce the bit error rate in a cooperative system by employing it in the Orthogonal frequency-division multiplexing (OFDM) cooperative system of the LTE network. This paper is a continuity to our previously published paper [17], which employed BCH code, but in a cooperative beamforming system. The primary contributions of this study are as follow;

1. Investigate the feasibility of using BCH and CC codes in the cooperative system of the LTE network while satisfying the particular regulatory conditions and ensuring that all specifications related to 3GPP and IMT [18] for the LTE-Advanced systems were fulfilled.
2. Implement a WINNER II channel model to represent a wireless channel between the nodes of the coded cooperative system and evaluate the performance of the suggestion model criteria with a direct link (no RN) and non-coded cooperative (with RN).
3. Determine the proper relay height in three scenarios. We have chosen the built-in scenarios of the WINNER channel model in three environments; suburban macro-cell (C1), urban macro-cell (B1), and rural micro-cell (D1).

This paper is organised in the following manner. Section 2 describes the Wireless Channel Models (WINNER II), which includes the geometry-based modelling of all radio channels, field patterns, and the antennae geometries. Section 3 briefly introduces the CC and BCH theoretical foundation that can be used in the OFDM cooperative system. Section 4 describes the LTE-Advanced cooperative system, while Section 5 describes the channel model parameters like Base Station (BS), Relay Node (RN), and the User Equipment (UE). Section 6 introduces the derived path loss models to be used in the selected environments. Section 7 presents the simulation system that used relay deployment processes and system parameters based on the WINNER channel model. Section 8 presents simulation results, and finally, Section 9 offers some recommendations for additional research and conclusions.

2. Wireless Channel Models Winner II

Many studies have used a single path loss model for the macro Evolved Node B (macro-eNB) attached to the UE connections, based on the conventional formulae used for the Non-Line-of-Sight (NLOS) propagation environment. A minor correction was proposed, which accounted for the use of a Line-of-Sight (LOS) component. This presumption was acceptable for the homogeneous networks, consisting of a constant site-to-site distance and a regular cell grid topology. On the other hand, using a single path loss model cannot present accurate information regarding the heterogeneous deployment since the macro-eNBs, and relay/pico/femto/remote radio head consist of varying transmitted powers, antenna heights, antenna gains, and down-tilts. However, the cell topology also differs in the Heterogeneous Network (HetNet), since it requires very sophisticated channel models for representing the propagation environment. The IMT-Advanced channel model was seen to be a geometry-based stochastic channel model, which evaluated the radio interface processes. The primary module framework was based on a WINNER II channel model consisting of a 100 MHz bandwidth with a 2-6 GHz central frequency. The WINNER channel model was a geometry-based stochastic model that helped in separating the propagation antennae and parameters. The channel parameters for the single snapshots were stochastically determined using statistical distributions that were extracted using the channel measurements. The field patterns and antenna geometries were defined using the model's user. The channel realisations were generated using the geometrical principle by including the contribution of the rays (i.e., plane waves) with particular small-scale parameters like power, delay, Angle of Arrival (AoA), and Angle of Departure (AoD). A superposition leads to the correlation between various temporal fading and antenna elements with a geometry-based doppler spectrum. [19] presented a transfer matrix for the MIMO channel as the following Equation 1.

$$H(t,\tau) = \sum_{m=1}^{m} H_m(t,\tau) \quad (1)$$

The above equation consists of the antenna array response matrices for transmitter (f_{tx}), for the receiver (f_{rx}), and a propagation channel response matrix (h_m) for the cluster m, in the following Equation 2 [20].

$$H_{u,s,m}(t,\tau) = \iint F_{rx}(\varphi)h_m(t,\tau,\emptyset,\varphi)F_{tx}^{T}(\emptyset)d_{\emptyset}d_{\varphi} \quad (2)$$

The cluster that was derived from the T_x antenna element *s*, to the R_x element, *u*, for the cluster, *n* in the following Equation 3 [21]:

$$H_{u,s,m}(t,\tau)(t,\tau) = \sum_{n=1}^{N}\begin{bmatrix}F_{rx,u,V}(\varphi_{m.n})\\F_{rx,u,H}(\varphi_{m.n})\end{bmatrix}^{T}\begin{bmatrix}\alpha_{m,n,VV} & \alpha_{m,n,VH}\\\alpha_{m,n,HV} & \alpha_{m,n,HH}\end{bmatrix}\begin{bmatrix}F_{tx,s,V}(\emptyset_{m.n})\\F_{tx,s,H}(\emptyset_{m.n})\end{bmatrix} \times e^{(j2\pi\lambda_0^{-1}(\overline{\emptyset_{m,n}}\cdot\overline{r_{rx,u}}))}e^{(j2\pi\lambda_0^{-1}(\overline{\varphi_{m,n}}\cdot\overline{r_{rx,s}}))} \times e^{j2\pi v_{m,n}t}\delta(\tau-\tau_{m,n}) \quad (3)$$

$F_{rx,u,V}$ and $F_{rx,u,H}$ are the antenna element for *u* field patterns in the vertical and horizontal polarisations, respectively. Furthermore, $\alpha_{m,n,VV}$ and $\alpha_{m,n,VH}$ are the complex gains for the vertical-to-vertical and horizontal-to-vertical polarisations for the ray *m, n,* respectively, whereas λ_0 represents the wavelength of the carrier frequency; $\overline{\emptyset_{m,n}}$ denoted the AoD unit vector; while $\overline{\varphi_{m,n}}$ represents the AoA unit vectors. $\overline{r_{rx,u}}$ and $\overline{r_{rx,s}}$ were seen to be the location vectors for the elements *u* and *s*, respectively. $v_{m,n}$ indicates the Doppler frequency component for the *m*, *n* ray. When the radio channel was modelled as a dynamic model, the above small-scale parameters varied according to time, *t*.

3. Coded Techniques

In this section, the CC and BCH coding techniques in the encoder and decoder used in an LTE-Advanced cooperative system are explained briefly.

3.1 Convolutional Coding (CC) Technique

Studies have used the convolutional coding process [22], [23] to reduce the likelihood of an erroneous transmission over the communication channels affected by the noise. An encoder is provided with a binary input, which is shifted into shift register *k*-bits. N-bits are seen to be the output bits for every input value of *k*. A convolutional encoder can be described in terms of generators, i.e., *n* vectors (having an *Lk* length) describe the chosen taps from a shift register that are mod-2 summed. Here, the values were $n = 2$; $k = 1$ and $L = 3$. The [1 7] octal generator was used, while the code rate (k=n) was 1/2, as presented in Fig. 1. The encoding data can be collected after the input data was passed through a convolutional encoder, as described in Fig. 1. Convolutional encoder showed a $2^{k(l-1)} = 4$ state, where *n* denoted the number of outputs; *k* indicated the number of inputs, while *L* was a constraint length.

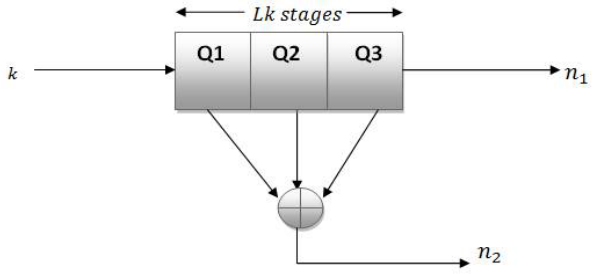

Fig. 1 - Convolutional encoder with a code rate of 1/2 generator matrix [1 7] octal

The convolutional decoder that implemented the Viterbi algorithm similar to the maximum likelihood criterion was used in this study due to the dependency on selecting correct decoded data corresponding to the minimal Hamming distance for every frame.

3.2 Bose-Chaudhuri-Hocquenghem (BCH) Coding Technique

In this process, the BCH encodes block created a BCH code using a message length, i.e., K=5; while the codeword length, N=15. The input should contain the defined K elements exactly. The output represented the vector with length, N. N is represented in the form of $2^{(M-1)}$, and M is an integer ≥3. For a specified codeword length of N, a specific message length of K was valid for the BCH code.

Furthermore, the BCH decoded block recovered the binary message vector from the binary BCH codeword vector. The primary two parameter values in the block have to be matched with the parameters described in a respective BCH encoder block to ensure proper decoding. The input is the binary codeword vector, while the subsequent binary message vector represents the output. It was noted that when the BCH code had a codeword length of N and message length of K, the input had a length of N while the output has the length K. However, if the input was frame-based, then it should be the column vector. Output 2 was the number of errors that were detected when the codeword was decoded. The negative value of the integer indicated that this block detected a higher number of errors compared to what it could correct using the coding scheme. The sample time for the input and the output signals was the same.

4. System Description

This study was conducted in 3 phases. Phase 1 is developing an LTE-Advanced non-cooperative system, and Phase 2 is developing an LTE-Advanced cooperative system. Finally, in Phase 3, the development of the coded LTE-Advanced cooperative system. The LTE-Advanced non-cooperative system was developed as the benchmark system to test the proposed coded LTE-Advanced cooperative system, which used the DAF protocol. The proposed LTE-Advanced cooperative system operated in the complete full-duplex mode, where simultaneous signal transmission or reception can be realized using the same transceiver during the downlink.

The coded LTE-Advanced cooperative system used CC or BCH codes that included the sender, relay, and destination units. In a sender unit, the user sends a text message as input information. This input is applied in a binary bit form to an ½ rated convolutional encoder [12]. Fig. 2 presents the simulated coded cooperative system block diagram.

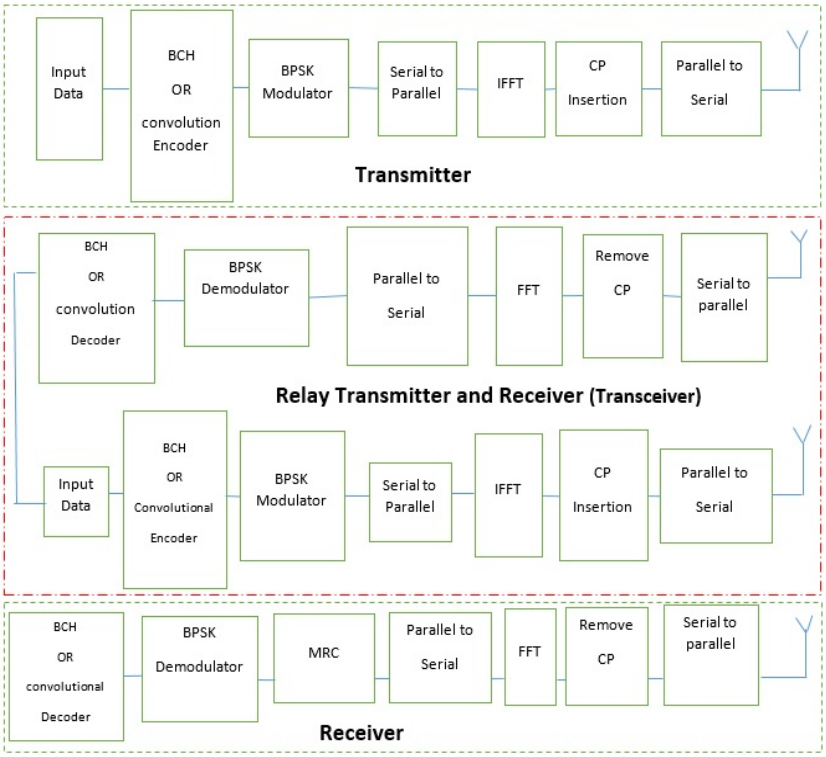

Fig. 2 - Block diagram of the coded OFDM cooperative system

The convolutionally-encoded bits were digitally modulated using a Binary Phase Shift Keying (BPSK) process. Once the serial-to-parallel conversion was concluded, all symbols were fed to the OFDM modulator that carried out an Inverse Fast Fourier Transform (IFFT) process on every OFDM block, 1024 symbols/subcarriers long. This was followed by the Cyclic Prefix (CP) of length, Lcp, which contained a copy of the last Lcp with parallel samples. After that, the derivation of parallel-to-serial converted output with 1024-point IFFT. The CP was seen to be a guard interval that could eliminate the interferences between the OFDM symbols. The resultant OFDM symbols having a length of 1024+Lcp were transmitted from the transmitting antenna. The receiver received 2 signals at the destination, where one was transmitted

directly from the sender unit, while the second was transmitted via the relay unit. The relay unit received a single signal that was transmitted from the sender unit, which was processed and retransmitted under DAF relaying protocols. At the destination, the two signals were combined with the help of different combining techniques.

Furthermore, the transmitted signal from the sender unit with a higher strength compared to the noise signal was retrieved. This retrieved signal was de-mapped through various sections of an OFDM demodulator and was convolutionally decoded for recovering the transmitted text message. Again, this processing is rerun after replacing ½ rated convolutional encoded/decoded with the BCH encoder/ decoder at sender, relay, and destination units [15, 5].

5. Channel Model Application

Here, the channel model for cooperative strategy was applied in three different environments, i.e., suburban macro-cells, urban macro-cells, and rural micro-cells. This cooperation strategy was modelled in two phases. In the first phase, the source broadcasts the information to the destination unit. The data is simultaneously received by a relay unit (owing to broadcast), as described in Fig. 3. In the second phase, the relay helps the source to forward or retransmit the information to a destination unit. Phase 1 describes the general relay channel, where the source transmitted the information using Power, P1, while the relay transmitted the information using Power, P2. A scenario has been investigated where the source and relay transmitted the information in Phase 2. Also, the relay unit helps the source by retransmitting and forwarding all information to a destination unit.

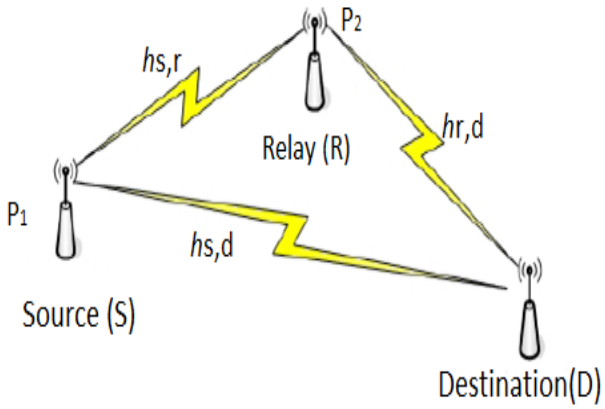

Fig. 3 - A cooperative system

To represent Phase 1 in the form of an equation; received signals; Y_{sd} and Y_{sr} at the destination and relay units, are written respectively as the following Equation 4 and 5:

$$Y_{sd} = \sqrt{P}h_{sd}x + n_{sd} \quad (4)$$

$$Y_{sr} = \sqrt{P}h_{sr}x + n_{sr} \quad (5)$$

P represents the transmitted power at source; x is a transmitted information symbol; n denotes the additive noise, while h ss the channel fading between the nodes, i.e., the Rayleigh flat fading channels. h is mathematically modelled as the complex Gaussian random variable. The real and imaginary parts were a 0 mean Independent variable and the Identically Distributed (IID) Gaussian random variable. Hence, the Equation 6:

$$Y_{rd} = h_{rd}q(Y_{sr}) + n_{rd} \quad (6)$$

where function $q(\cdot)$ was dependent on the processing that was implemented at the relay node. Based on the knowledge of all channel coefficients (between source and destination, or relay and destination), the destination unit detected the transmitted symbols after combining all received signals from the source and relay units. The destination unit receives two copies of a transmitted signal via the source link, Y_{sd} (4), and relay link, Y_{rd} (6). Different techniques could be used for combining the signals received at the destination unit. The optimisation process which maximises the general SNR value was the Maximum ratio Combiner (MRC). The MRC combining process was a coherent detector that required the

knowledge of all the channel coefficients. Hence, based on this knowledge of h_{sd} , h_{sr} and h_{rd} channel coefficients, MRC detector output at the destination was described as Equation 7.

$$Y = A\,Y_{sd} + B\,Y_{rd} \tag{7}$$

A and *B* were the combining factors that were designed for maximising the combined SNR. These factors can be designed using the detection theory principles on the signal space. Since the AWGN noise terms can span the entire space to minimize noise effects, the detector projects the received signals and the desired signal space. The Y_{sd} and Y_{rd} signals must be projected sequentially along the direction after the noise variance terms were normalised in the received signals. Hence, *A* and *B* were expressed as in Equation 8.

$$B = \frac{\sqrt{P_2}h_{r,d}^*}{N_0} \; and \; A = \frac{\sqrt{P}h_{s,d}^*}{N_0}, \tag{8}$$

6. Path Loss Model

The path loss model deals with the large-scale or long-term variations noted on an average strength of the received signals based on the variation of distances between the receiver and transmitter. This path loss indicates the speed at which the strength of the received signal decreases with the distance. The popular path loss model includes the free-space path loss model, where the mean received signal strength was inversely proportional to the distance square (i.e., the strength of the received signal decreased 4-times when the distance was doubled). In the case of terrestrial wireless communication, this signal strength decreased very rapidly. Furthermore, the path loss between a receiver and transmitter was based on a path loss exponent dependent on the environment. The path loss value was 2 in rural areas or free space, 2-3 in suburban regions, around 4 in urban areas, and not deterministic in the case of irregular terrain. A high path loss value indicates a faster drop in the signal strength, with an increasing distance value. In this study, the empirical model is used for modelling path loss [20].

Various path loss models for differing WINNER scenarios were developed depending on the measurement values derived from the literature. These models were based on the following Equation 9 [24].

$$PL = A\,log_{10}\,d + B + C\,log_{10}\frac{f_c}{5} + K \tag{9}$$

d (in meter) denotes the distance between the receiver and transmitter; f_c [in GHz] represents the system frequency, and *A* indicates the fitting parameter, including a path-loss exponent. B represents an intercept in the above form, which was a fixed value based on the empirical observations and was estimated using the free space path loss based on the reference distance and the environment-dependent constant. Factor *C* denoted the path loss frequency dependence, whereas *K* was an optional environment-related term dependent on the situation. These models could be applied at varying antenna heights and frequency values ranging between 2 and 6 GHz. In [25], the researchers described the estimated values based on the empirical observations for *A, B, C*, and *K* variables. A free-space path loss, PL_{free}, was expressed as Equation 10.

$$PL_{free} = 20\,log_{10}\,d + 46.4 + 20\,log_{10}\frac{f_c}{5} \tag{10}$$

Both Equations 9 and 10 serve as the basic path loss formula, which will be expanded according to different WINNER channel models in Section 6.1. The path loss models used in the different situations with the WINNER channel model were based on the measured data derived at 2 and 5 GHz frequencies. The models were extended to the arbitrary frequencies ranging between 2 and 6 GHz, with the help of a path loss intercept and path loss frequency dependencies.

6.1 Scenario C1: Suburban Macro-Cell Scenario with Relay factors

The suburban macro-cell scenario C1 included in WINNER can be described in the following manner. The suburban macro-cell (C1) situation values were determined at a central frequency value of 2.5 GHz, where the residences were at a lower height than the town centre's building. The heights of these houses varied between 3 to 6 storeys. The area also includes parks, parking spaces, and trees which lined the streets between these houses. The effective height of the antenna was presumed as the actual height since the suburban areas showed a relatively low vehicular density. Based on the

parameters that were proposed for the WINNER II model, a path loss Equation 11 could be written for this situation as follow.

$$PL_{los} = 40.0\ log_{10}\ (d[m]) + 11.65 - 16.2log_{10}\ (h_{BS}[m]) - 16.2log_{10}\ (h_{MS}\ [m]) + 3.8log_{10}(f\ [GHz]/5.0) \quad (11)$$

d represents the distance between a receiver and transmitter; $d_{BP} < d < 5km$, $d_{BP} = 4h_{BS}h_{RS}fc$, , h_{BS} the BS height; while h_{RS} denotes the relay station height; h_{MS} the user equipment height; f is a carrier frequency; c the light velocity in a vacuum. In this case, h_{BS} = 25 m; h_{MS} =1.5 m and h_{RS} =5, 15, and 20 m.

6.2 Scenario B1: Urban Micro-Cell Scenario with Relay Scenarios

In the case of an urban micro-cell, B1, the height of the antennae at the Base Station (BS) and User Equipment (UE) were presumed to be lower than the height of the neighbouring buildings. The antennas were presumed to be in an outdoor area where the streets were laid into a Manhattan-like grid. These streets were classified as "the main street", where a LOS was noted from this location to BS. Exception in the situations where LOS was blocked temporarily by the traffic like trucks or buses. The streets which intersected the main streets were called perpendicular streets, and others that ran parallelly to the main street were called parallel streets. Regarding the RN in an urban micro-cell scenario, the relay station was situated at the intersection between the branching and main streets, as presented in Fig. 4., with the help of the relay deployment and combination process depicted in Section 7. The path-loss is given in Equation 12.

$$PL_{los} = 40.0\ log_{10}\ (d[m]) + 9.45 + 17.3log_{10}\ (h'_{BS}\ [m]) + 17.3log_{10}\ (h'_{MS}\ [m]) + 2.7log_{10}(f\ [GHz]/5.0) \quad (12)$$

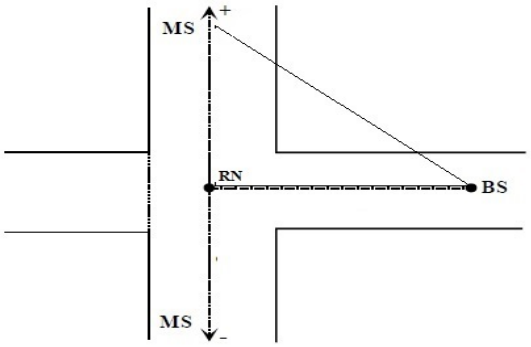

Fig. 4 - An urban micro-cell scenario

d denotes the distance between a receiver and transmitter; $d'_{BP} < d < 5km$, $d'_{BP} = 4h'_{BS}h'_{RS}fc$, h'_{BS} represents the BS antenna height (real h_{BS} was presumed as 1.5 m), h'_{RS} the effective antenna height of a relay station (real value was presumed as 1.5 m), h'_{MS} indicates the effective UE antenna height of a relay station, (real h_{RS} was assumed as 1 m), f denotes the carrier frequency; while c is the light velocity in a vacuum; σ was the standard deviation. The values of h_{BS} = 10 m, h_{MS} =1.5 m, h_{RS} = 3 to 5 m, and $\sigma = 3$ dB.

6.3 Scenario D1: Rural Macro-Cells with Relay Scenarios

The D1 propagation scenario represented the radio propagation in larger areas (with the radius of the area up to 10 km) with a lower building density. The AP antenna height ranged between 20 and 70 m, which was higher compared to the average height of the buildings). As a result, LOS conditions were noted in the overall coverage area. However, if the User Equipment (UE) was located within a vehicle or building, an extra penetration loss was noted and modelled in the form of a frequency-dependent constant. The location of the AP antenna location was fixed in this situation, while the velocity of the UE antenna ranged between 0 and 200 km/h

In a WINNER Phase I case, the measurement was carried out in the flat rural area near Oulu, Finland, with two frequency values, i.e., 2.45 and 5.25 GHz, while the AP antenna height ranged between 18 m and 25 m. The result is Equation 13.

s

$$PL_{los} = 10.5 + 40.0\ log_{10}\ (d_1[m]) - 18.5log_{10}\ (h_{BS}\ [m]) - 18.5log_{10}\ (h_{MS}\ [m]) + 1.5log_{10}(f\ [GHz]/5.0) \quad (13)$$

7. Simulation Set-up of the System

As the WINNER channel model was delivered solely in the physical layer, the designed simulator was seen to be a physical level simulator. The major components which were used for designing the simulator included the RN, BS, UE, and the scenarios. It is essential to implement a multi-hop environment for a simulator, where the relay unit was located between the UE and BS.

7.1 Rural Macro-Cells with Relay Scenarios

Relay transmission is a form of collaborative communication, where the RN forwards user data from the neighbouring UEs to local BS. This relay is restricted to the combination of the UE (i.e., receiving part) and BS (i.e., transmission part). Hence, a deploying relay is described as deploying a component of UE and BS in this environment, as described in Fig. 5.

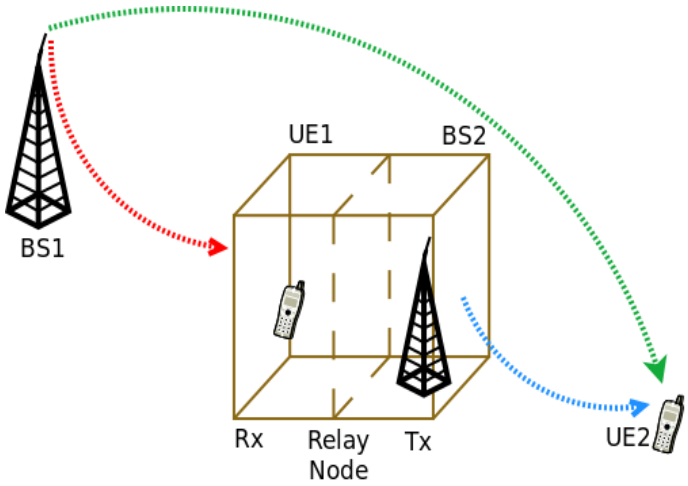

Fig. 5 - A relay deployment based on the combination of a BS and UE

The design included 2 BS, i.e., BS1 and BS2, and 2 UEs, i.e., UE1 and UE2. An RN was constructed using a pair of BS2 and UE1. A Relay link is described as a link between UE1 and BS1, while an access link is formed between the BS2 and UE2. Furthermore, the link noted between the BS1 and UE2 was called a direct link. The signal from the BSI to the UE2 was transmitted with the help of UE1 and BS2, which acted as the relay for BS1. In the case of a multi-hop network, several BS-UE pairs were introduced at the relay position. For deploying the RN, the procedure is described below:

1. In Step 1, set the positions of the BS1 and the antenna array orientations for BS1.
2. In Step 2, set the UE2 position and the antenna array orientations for UE2.
3. For constructing the RN, the UE1 and BS2 were added, as shown in Fig. 5. All array characteristics and array orientations for the BS2 and UE1 were kept the same.
4. After that, define the UE×BS pairing matrix for constructing the RN. In a cooperative system scenario (with relay), the form of pairing matrix A was established, as the following Equation 14.

$$A = \begin{bmatrix} BS1 & BS2 & BS1 \\ UE1 & UE2 & UE2 \end{bmatrix} = \begin{bmatrix} 1 & 2 & 1 \\ 3 & 4 & 4 \end{bmatrix} \quad (14)$$

In this matrix, based on the design described in Fig. 5, Node 1 represented BS1, Node 2 represented UE1, Node 3 represented BS2, while Node 4 represented UE2. A relay link linked Nodes 1 and 3; an access link linked Nodes 2 and 4, while a Direct link linked Nodes 1 and 4. BS2 and UE1 constituted a pair, while no pairing was noted between the BS1-UE1, BS1-UE2, or BS2-UE2, before the RNs were constructed. All the radio links were then generated at the same time

5. Finally, the channel segments were simulated.

7.2 The Output of All Link Parameters

The output for earlier simulation includes many parameters. In this simulation, the number of links (K), paths in every link (N), and sub-paths in every path (M) were defined, and the output parameters noted in the simulation were:

1. Delays: $K \times N$ matrix for the path delays (s).
2. AODs and AOAs distribute uniformly between -180° to 180°.
3. Path losses: These were represented using the ($K \times 1$) matrix for every scenario. The formula for measuring path loss can be referred to in Section 6. It includes a coefficient multiplied by transmitted power.
4. Distances between all stations were represented using a $K \times 1$ matrix.
5. Shadow fading losses were measured using a linear scale. They were represented using the K ×1 matrix and included a coefficient multiplied by mean path loss.

7.3 Evaluation of the BER Results

A link-level simulation was performed to study the BER in 3 different environments, as mentioned in Section 6. The OFDM multiplexing technique was considered, while stimulation parameters included in the simulation to evaluate the BER are presented in Table 1. Fig. 6. presents the algorithm for the coded OFDM simulator and relay construction for some SNR values. The algorithm identifies and specifies initial set-ups like the antenna array and orientation, chosen scenario parameters, and BS, UE, and RN position. This follows with the generation of all the radio links based on the WINNER ll channel model to compute the power of the relay link and BER based on different coded OFDM systems. The processes were repeated 10,000 times, and finally, average BERs were concluded.

Table 1 - Simulation parameters

System Parameters	Definition
Channel Bandwidth	20 MHz
Carrier Frequency	2.5 GHz
Channel Model used	WINNER II
Path Loss models	Line of Sight (LOS)
UE height	1.5 m
BS height	C1 (125 m), D1 (30 m) and B1 (10 m)
BS transmitted power	46 dBm
BS antenna gain	14 dBi
BS noise figure	5 dB
RN height	Between 5, 15, 20 & 25
RN noise figure	7 dB
UE height	1.5 m
UE numbers	1 (single user)
UE noise figure	7 dB
System bandwidth	20 MHz
Data modulation	BPSK
BCH Coding	[15,5]
Convolutional Coding	[1 7], rate=1/2
Cyclic prefix	256 samples
Transmitter IFFT size	1024
Thermal noise level	-174 dBm
Number of iterations	10^4

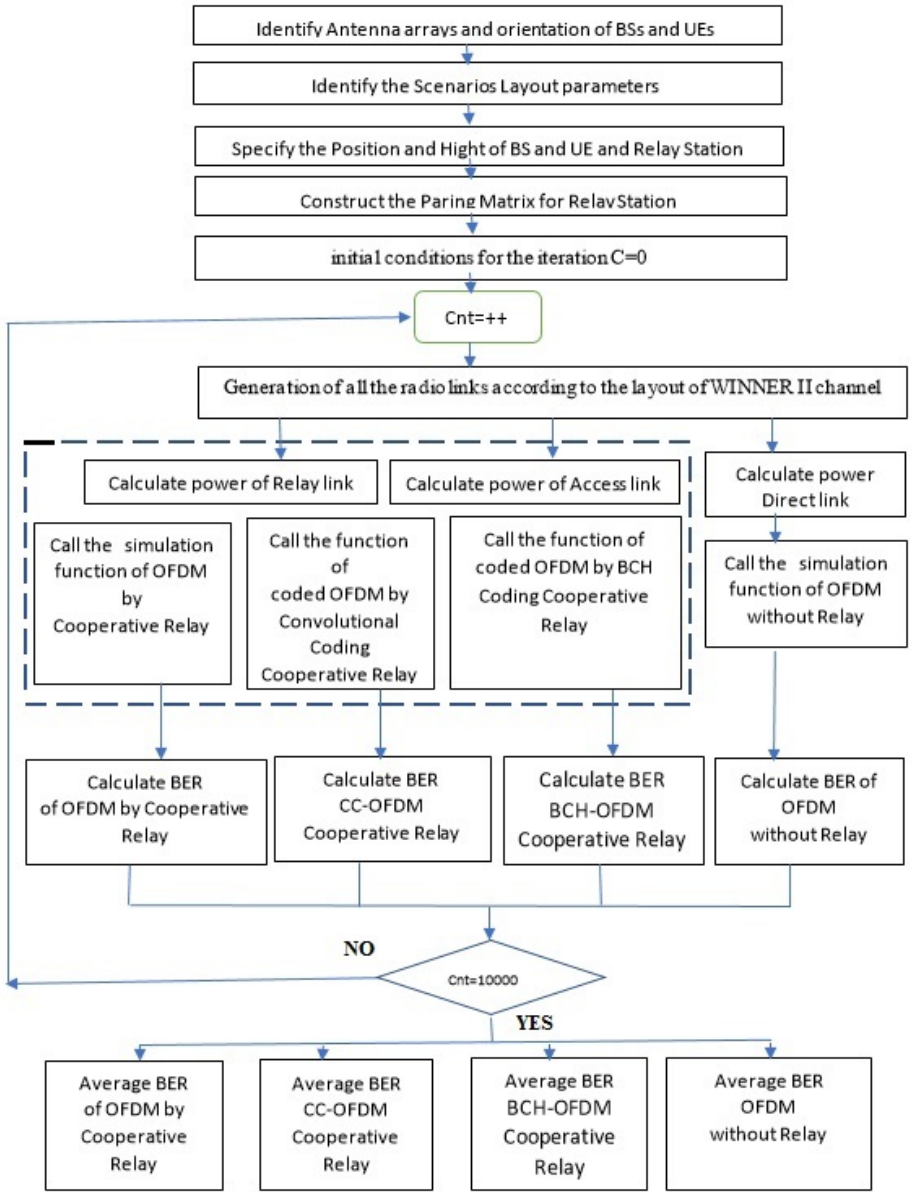

Fig. 6 - Algorithm for the coded OFDM simulator

8. Simulation Results

All systems included in Section 4 were simulated with the help of the Matlab codes. Fig. 7. depicts the suburban macro-cell scenario, C1 performance of OFDM evaluation in a DAF cooperative system, OFDM in the direct link, CC-OFDM in a DAF cooperative system, and the BCH-OFDM in a DAF cooperative system. Results showed better BER performance with the BCH code. Hence, for achieving a BER value of $\approx 10^{-4}$, SNR needed in a cooperative system of BCH-OFDM was 15 dB less than that needed for a direct OFDM link, 2.5 dB less than that needed for a cooperative system CC-OFDM, or 5 dB less than that needed for a cooperative system OFDM.

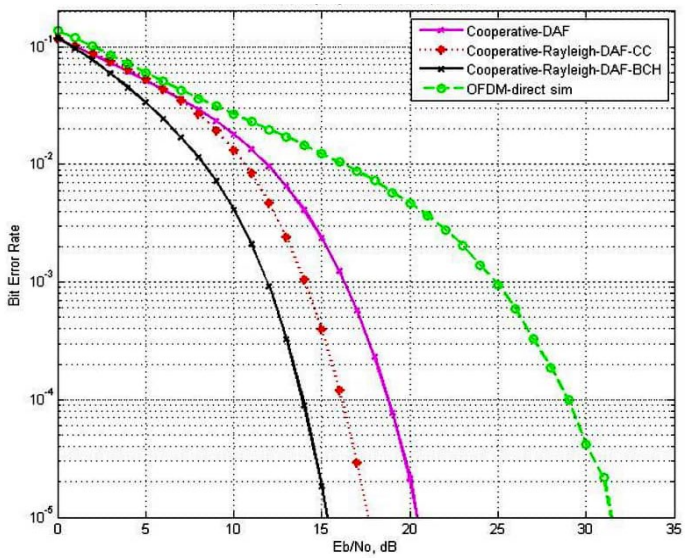

Fig. 7 - BER performance of OFDM in the direct link, OFDM in cooperative DAF, CC-OFDMA in cooperative DAF and BCH-OFDM in cooperative DAF for scenario C1 (suburban)

In a suburban macro-cell scenario, C1, the BER performance of a cooperative system with the BCH-OFDM process was investigated at differing relay heights. Fig. 8. indicated that the system's performance could be improved if the Relay height was 15 m. For achieving a BER value of $\approx 10^{-4}$, the SNR needed for a Relay height value of 15 m was 4 dB less than that needed for a relay height of 20 m, or 7.5 dB less than that needed for a relay height of 5 m.

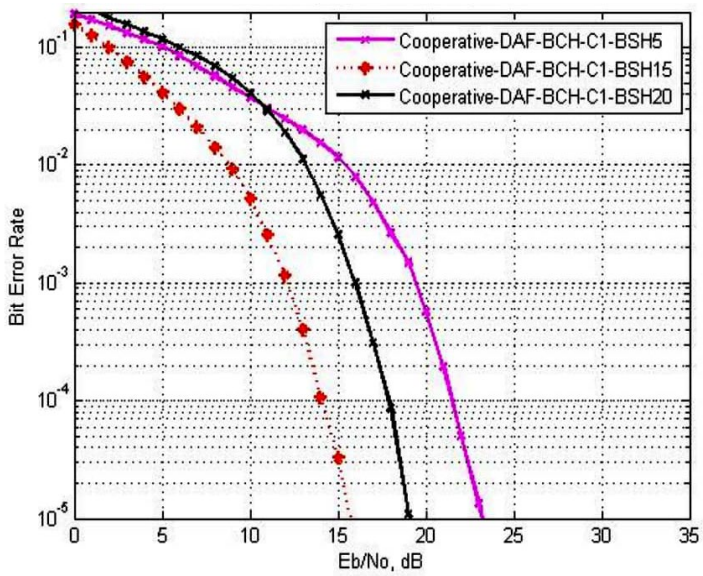

Fig. 8 - BER performance of BCH-OFDM in a cooperative DAF with different relay heights in scenario C1 (suburban)

In the case of a suburban macro-cell scenario, C1, Fig. 9. presents the results of the BER performance of a cooperative system with the BCH-OFDM process at differing relay distances. The system performance was significantly improved if the relay was situated between the UE and BS. Hence, for achieving a BER of $\approx 10^{-4}$, the SNR needed for a Relay distance of 500 m was 3 dB less than that needed for a relay distance of 200 m, or 9 dB less than that needed for a relay distance of 800 m from BS.

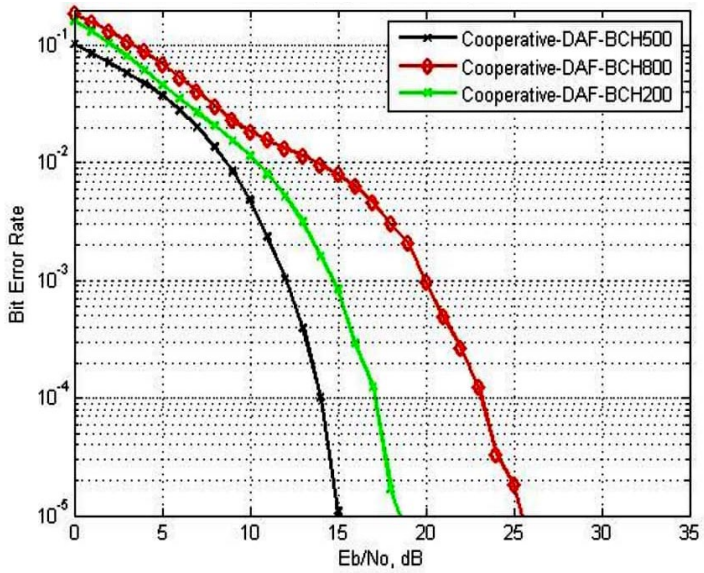

Fig. 9 - BER performance of the BCH-OFDM system using a cooperative DAF with varying relay distances in scenario C1 (suburban)

In the case of a rural macro-cell Scenario D1, the BER performance of a cooperative system with the BCH-OFDM technique was also investigated at differing relay heights. Fig. 10. indicated that the performance of the system could be improved if the Relay height was 15 m. Hence, for achieving a BER of $\approx 10^{-4}$, the SNR needed for a Relay height of 15 m was 5 dB less than that needed for a relay distance of 25 m, or 12.5 dB less than that needed for a relay height of 5 m.

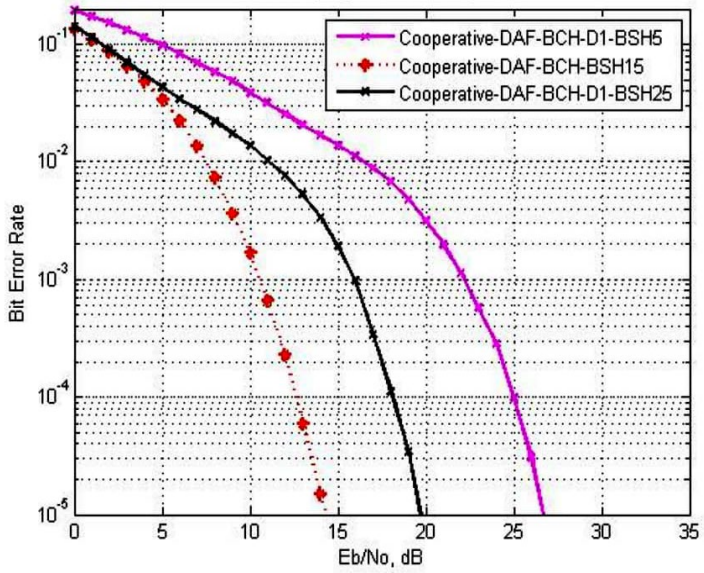

Fig. 10 - BER performance of BCH-OFDM in a cooperative DAF with differing relay heights in scenario D1 (rural)

In an urban macro-cell scenario B1, the BER performance of a cooperative system using the BCH-OFDM process was investigated at differing relay distances. They altered the RN and the UE location. RN was placed at the intersection of the branch street and main street, while the UE was placed along this main street, as shown in Fig. 4. Results indicated that the system's performance could be improved if the distance between the RN and BS or the distance between the UE and RN was short, as indicated in Fig. 11. Hence, for achieving a BER of $\approx 10^{-4}$, the SNR needed for a Relay distance of 100 m and 250 RN-UE and BS-RN was 7 dB less than that noted for the respective distances of 3000 m and 500 m.

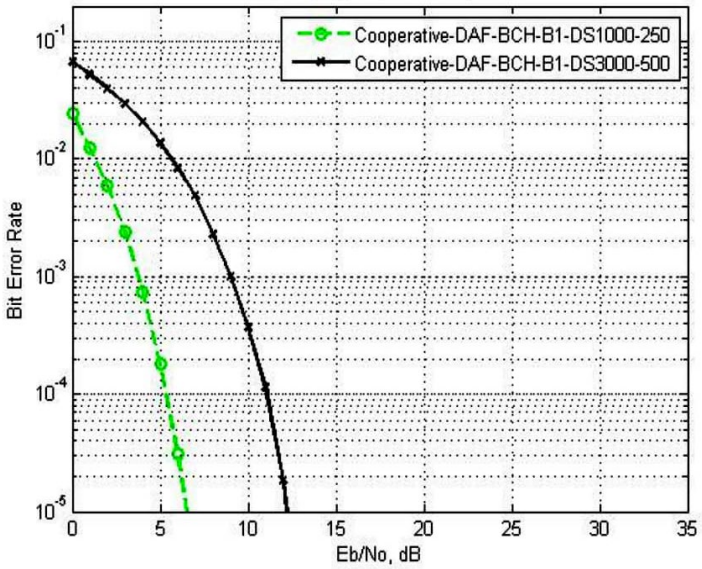

Fig. 11 - BER performance of the BCH-OFDM in a cooperative DAF with differing relay distances from the UE and BS in scenario B1 (urban)

Based on the results generated previously, Table 2 summarizes the comparison based on different relay heights and varying relay distances. The table highlighted the best configuration based on various deployment scenarios with the performance gain, compared to the other considered height and distances configurations. It can be observed that the vast performance gain can be achieved under the deployment Scenario B1 (Urban), with the highest performance gain of 7 dB.

Table 2 - Summary of performance gain and best relay configuration based on considered deployment scenarios

Scenario	Best Relay Configuration	Performance Gain, dB
Scenario C1 (Suburban)	height = 15 m	3.5
Scenario C1 (Suburban)	distant = 500 m	3.5
Scenario D1 (Rural)	height = 15 m	6
Scenario B1 (Urban)	distant = 1000 m	7

9. Conclusion

We have investigated the performance of coded LTE-Advanced cooperative systems based on two different coding schemes, known as convolutional code (CC) and Bose-Chaudhuri-Hocquenghem (BCH), to further improve the BER. Both of the coding techniques were simulated in the WINNER II wireless channel model under three different scenarios; B1 (urban-micro cell), C1 (suburban macro-cell) and D1 (rural macro-cells), while the RN is in the stationary condition at various heights. The results have shown that the LTE-Advanced system employing a cooperative system with BCH code has superior BER performance than those with CC. The BER gain achieved by the BCH-based cooperative LTE-A can be explained by the capability of the BCH code to transmit an independent copy of wireless signals, which promotes higher spatial diversity to minimize the fading effect. Also, the height of the RN plays a significant role in influencing the BER performance. The results have shown that the RN height must be lower than BS in a coded LTE-Advanced cooperative system to ensure minimum BER loss. Future work will consider RN in differing locations based on the location of user equipment and consider the latest progress in the Fifth Generation or 5G transmission based on the 3GPP-Release 15 and 16 standards.

References

[1] Lai, I. W., Shih, J. W., Lee, C. W., Tu, H. H., Chi, J. C., Wu, J. S., & Huang, Y. H. (2019). Spatial permutation modulation for multiple-input multiple-output (MIMO) systems. IEEE Access, 7, 68206-68218.

[2] Shen, D., Gao, Z., Liao, X., & Sun, X. (2018, December). Secrecy Enhancement for Multiple-Input Multiple-Output OFDM with Index Modulation. In 2018 IEEE International Conference on Communication Systems (ICCS) (pp. 142-146). IEEE.
[3] El Maammar, N., Bri, S., & Foshi, J. (2018). Performances Concatenated LDPC based STBC-OFDM System and MRC Receivers. International Journal of Electrical & Computer Engineering (2088-8708), 8(1).
[4] Shaheen, F., Butt, M. F. U., Agha, S., Ng, S. X., & Maunder, R. G. (2019). Performance analysis of high throughput map decoder for turbo codes and self concatenated convolutional codes. IEEE Access, 7, 138079-138093.
[5] Hunter, T. E., & Nosratinia, A. (2002, June). Cooperation diversity through coding. In Proceedings IEEE International Symposium on Information Theory, (p. 220).
[6] Cao, Y., & Vojcic, B. (2005, March). Cooperative coding using serial concatenated convolutional codes. In IEEE Wireless Communications and Networking Conference, 2005 (Vol. 2, pp. 1001-1006).
[7] Prabagarane, N., Al-Hilfi, H. M. T., & Tamilarasi, M. (2019). Performance of cooperative diversity aided TF-spread MC-DS-CDMA with preprocessing. Computers & Electrical Engineering, 78, 504-519.
[8] Xu, J., Yang, W., Tan, Y., & Kim, Y. I. (2018). A joint cross-layer transmission design with time-frequency coded cooperation HARQ for underground coal mine MC-CDMA WSNs. Wireless Networks, 24(5), 1655-1666.
[9] Vishvaksenan, K. S., Rajmohan, R., & Kalaiarasan, R. (2017, April). Multi-carrier IDMA system for relay aided cooperative downlink communication with transmitter preprocessing. In 2017 International Conference on Communication and Signal Processing (ICCSP) (pp. 2206-2210). IEEE.
[10] Xu, L., Wang, H., Liu, Y., & Gulliver, T. A. (2019). Performance Analysis of Mobile Multiuser Cooperative Networks with TAS Schemes. Journal of Signal Processing Systems, 91(5), 503-509.
[11] Huang, W. J., Hong, Y. W. P., & Kuo, C. C. J. (2008). Relay-assisted decorrelating multiuser detector (RAD-MUD) for cooperative CDMA networks. IEEE Journal on Selected Areas in Communications, 26(3), 550-560.
[12] Fadhil, M., Ismail, M., Saif, A., Othman, N. S., & Khaleel, M. (2014, April). Cooperative communication system based on convolutional code CDMA techniques. In 2014 IEEE REGION 10 SYMPOSIUM (pp. 594-599).
[13] Joundan, I. A., Nouh, S., Azouazi, M., & Namir, A. (2019). A new efficient way based on special stabilizer multiplier permutations to attack the hardness of the minimum weight search problem for large BCH codes. International Journal of Electrical & Computer Engineering (2088-8708), 9(2).
[14] Boiko J, Eromenko O. Signal Processing in Telecommunications with Forward Correction of Errors. Indonesian Journal of Electrical Engineering and Computer Science. 2018; 11(3): 868-877.
[15] Waheed, M., Ahmad, R., Ahmed, W., Drieberg, M., & Alam, M. M. (2018). Towards efficient wireless body area network using two-way relay cooperation. Sensors, 18(2), 565.
[16] Pyndiah, R. M., Guilloud, F., & Amis, K. (2010, September). Multiple source cooperative coding using turbo product codes with a noisy relay. In 2010 6th International Symposium on Turbo Codes & Iterative Information Processing (pp. 98-102). IEEE.
[17] Fadhil, M., Abdullah, N. F., Ismail, M., Nordin, R., Ciftlikli, C., & Al-Obaidi, M. (2019). Maximizing signal to leakage ratios in MIMO BCH cooperative beamforming scheme. International Journal of Electrical and Computer Engineering, 9(5), 3701.
[18] Docomo, N. T. T. (2004). Proposed Study Item on Evolved UTRA and UTRAN. 3GPP TSG RAN, TD RP-040461.
[19] Cho, Y. S., Kim, J., Yang, W. Y., & Kang, C. G. (2010). MIMO-OFDM wireless communications with MATLAB. John Wiley & Sons.
[20] Bultitude, Y. D. J., & Rautiainen, T. (2007). IST-4-027756 WINNER II D1. 1.2 V1. 2 WINNER II Channel Models. EBITG, TUI, UOULU, CU/CRC, NOKIA, Tech. Rep., Tech. Rep.
[21] Ahmadi, S. (2013). LTE-Advanced: a practical systems approach to understanding 3GPP LTE releases 10 and 11 radio access technologies. Academic Press.
[22] Dhaliwal, S., Singh, N., & Kaur, G. (2017, February). Performance analysis of convolutional code over different code rates and constraint length in wireless communication. In 2017 International Conference on I-SMAC (IoT in Social, Mobile, Analytics and Cloud)(I-SMAC) (pp. 464-468). IEEE.
[23] Chung, C. C., Sheng, D., & Li, M. H. (2020). Design of a human body channel communication transceiver using convolutional codes. Microelectronics Journal, 104783.
[24] Hamid, M. D. (2014). Measurement based statistical model for path loss prediction for relaying systems operating in 1900 MHz band (Doctoral dissertation).
[25] Yuan, Y. (2013). Physical Layer Standardization of Release 10 Relay. In LTE-Advanced Relay Technology and Standardization (pp. 91-133). Springer, Berlin, Heidelberg.